Supporting Information

Supporting Information

Synergy between Silver-Copper Surface Alloy Composition and Carbon Dioxide Adsorption and Activation

Yifan Ye[1,2,3,#], Jin Qian[3,4,#], Hao Yang[4,5#], Hongyang Su[2,6], Kyung-Jae Lee[2,7], Ane Etxebarria[2,8,9], Tao Cheng[4,5,10], Hai Xiao[4,10], Junko Yano[1,11*], William A. Goddard III[4,10*], Ethan J. Crumlin[2,3*]

[1] Joint Center for Artificial Photosynthesis, Lawrence Berkeley National Laboratory, Berkeley, CA 94720, United States;

[2] Advanced Light Source, Lawrence Berkeley National Laboratory, Berkeley, CA 94720, United States;

[3] Chemical Sciences Division, Lawrence Berkeley National Laboratory, Berkeley, CA 94720, United States;

[4] Materials and Process Simulation Center, California Institute of Technology, Pasadena, CA 91125, United States;

[5]Institute of Functional Nano&Soft Materials (FUNSOM), Jiangsu Key Laboratory for Carbon-Based Functional Materials & Devices, Soochow University, Jiangsu, 215123, China;

[6] Hefei National Laboratory for Physical Sciences at the Microscale, University of Science and Technology of China, Hefei, Anhui 230026, P. R. China;

[7] Department of Physics and Photon Science, Gwangju Institute of Science and Technology (GIST), Gwangju 500-712, South Korea;

[8] Centre for Cooperative Research on Alternative Energies (CIC energiGUNE), Basque Research and Technology Alliance (BRTA), Alava Technology Park, Albert Einstein 48, 01510 Vitoria-Gasteiz, Spain;

[9] Department of Condensed Matter Physics, Faculty of Science and Technology, University of the Basque Country, UPV/EHU, Apdo 644, 48080 Bilbao, Spain;

[10] Joint Center for Artificial Photosynthesis, California Institute of Technology, Pasadena CA 91125, United States;

[11] Molecular Biophysics and Integrated Bioimaging Division, Lawrence Berkeley National Laboratory, Berkeley, CA 94720, United States.

# These authors contributed equally

***Corresponding Authors:** jyano@lbl.gov; wag@caltech.edu; ejcrumlin@lbl.gov

Supporting Information

Supplementary Information Contents:

Supporting Information

Computational Methods

1. Free energies calculations

Calculations for the gas phase molecules used the PBE functional (as implemented in Jaguar) with the D3 empirical correction for London dispersion. To obtain the total free energy, G = H−TS, for the gas molecules at temperature T, we add to the DFT electronic energy (E), the zero-point energy (ZPE) from the vibrational levels (described as simple harmonic oscillators), and the specific heat corrections in the enthalpy from 0 to T. The entropy (S), as a sum of vibrational, rotational and translational contributions, are evaluated from the same levels. To correct the free energy for pressure, we assume an ideal gas and add $RT\times\ln(P_2/P_1)$ with a reference pressure of P = 1 atm. For example, CO_2 gas at room temperature and 1atm would have a free energy correction of −0.25 eV, including ZPE (0.32 eV), translational entropy contribution (−0.42 eV), rotational entropy contribution (−0.15 eV) and almost negligible vibrational entropy contribution (−0.003 eV). All calculations assume the current experimental condition: $P(CO_2)$ = 300 mTorr, and $P(H_2O)$ = 150 mTorr. After the gas molecules adsorbed on the metal surface, their rotational and translational degrees of freedom are reduced to vibrational modes. The vibrational frequencies for surface adsorbents are calculated by allowing the adsorbed molecules and the top layer of metal to relax, with the bottom layers fixed. For these phonon calculations we used 10^{-6} eV energy convergence threshold to obtain reliable phonon frequencies (no negative eigenvalues.) To obtain the Free energy, G = H−TS, for the various equilibrium configurations, we used density functional perturbation theory (DFPT) to calculate the phonon density of states, which was used to calculate the ZPE, the temperature correction to the enthalpy, and the vibrational contributions to the entropy.[1-3]

2. Core Level Shift Calculations

There are two ways of calculating the change in core level energies implemented in VASP.[4] The simpler option (ICORELEVEL = 1) calculates the core levels in the initial state approximation, which involves recalculating the KS eigenvalues of the core states after a self-consistent calculation of the valence charge density. In the second option (ICORELEVEL = 2), electrons are removed from the core and the final state approximation is followed. Our previous studies found that the ICORELEVEL =1 leads to relative binding energy shift in good agreement with experimental XPS **accounting for the screening effect of metals**.

Supporting Information

Convergence test

Thickness of Ag substrates	E_{ad} (O=$CO_2^{\delta-}$)/ eV	G_{ad} (O=$CO_2^{\delta-}$)/ eV
4 layers	−0.73	−0.26
5 layers	−0.75	−0.28
6 layers	−0.81	−0.34
7 layers	−0.68	−0.21
Average	−0.74	−0.27

Table S1. Convergence test with Ag substrates of 4-7 layers. We found that all structures of adsorbed O = $CO_2^{\delta-}$ species are maintained, and the adsorption energy was on average −0.74 eV (E) and −0.27 eV (G), which was very close to the values that we obtained assuming the four-layer structures, which are −0.73 eV (E) and −0.26 eV (G). The four-layer model was sufficiently reliable to represent the properties of these periodic systems.

Supporting Information

Stability of $O{=}CO_2^{\delta-}$ on pure Ag and pure Ag unit with one Ag replaced by Cu at the first layer, second layer, and third layer.

Substrates	E_{ad} / eV	G_{ad} / eV	$E_{(O=CO2\delta- +Substrates)}$ / eV	deltaBE / eV
Surface O-Ag	-0.75	-0.28	/	0.00
Surface O-Ag-1st layer Cu	-0.55	-0.08	-274.25	0.34
Surface O-Ag-2nd layer Cu	-0.63	-0.16	-274.02	0.02
Surface O-Ag-3rd layer Cu	-0.57	-0.10	-273.98	0.01

Table S2. Stability of $O{=}CO_2^{\delta-}$ on pure Ag and pure Ag unit with one Ag replaced by Cu at the first layer, second layer and third layer.

We evaluated the adsorption energy for $O{=}CO_2^{\delta-}$ adsorption. For pure Ag, $G_{ad}(O{=}CO_2^{\delta-}) = -0.28$ eV; for 1 Cu surface dopant (in the 1st layer), $G_{ad}(O{=}CO_2^{\delta-}) = -0.08$ eV; for 1 Cu subsurface dopant (Cu at the 2nd layer), $G_{ad}(O{=}CO_2^{\delta-}) = -0.16$ eV; for 1 Cu placed in the third layer, $G_{ad}(O{=}CO_2^{\delta-}) = -0.10$ eV.

We include the total energy of $E(O{=}CO_2^{\delta-}$ +Substrates) (4th column in the **Table S2**) to account for different surfaces with $O{=}CO_2^{\delta-}$ adsorbed on different bimetallic substrates. We found that the $O{=}CO_2^{\delta-}$-Ag-1st-layer Cu has the most stable energy among bimetallic systems, which is 0.23 eV more stable than second- and third-layer Cu. We want to clarify that when calculating the stability of $O{=}CO_2^{\delta-}$ it is more reasonable to compare the $E(O{=}CO_2^{\delta-}$ +Substrates) (4th column in the **Table S2**) energetics rather than adsorption energy $E_{ad}(CO_2)$ or $G_{ad}(CO_2)$, because the adsorption energy is calculated by referencing to the oxidized surface. Our conclusion is that Cu atoms involved in the surface reaction and the bimetallic system is Ag-like, but indeed different from pure Ag due to this surface Cu atom. The final conclusion is that Cu atoms prefer to stay on the surface when adsorbents such as O and $O{=}CO_2^{\delta-}$ are present. Having Cu atoms buried inside the Ag matrix does not affect the adsorption geometry or the XPS BEs.

Supporting Information

Surface characterization using APXPS, a depth profile study

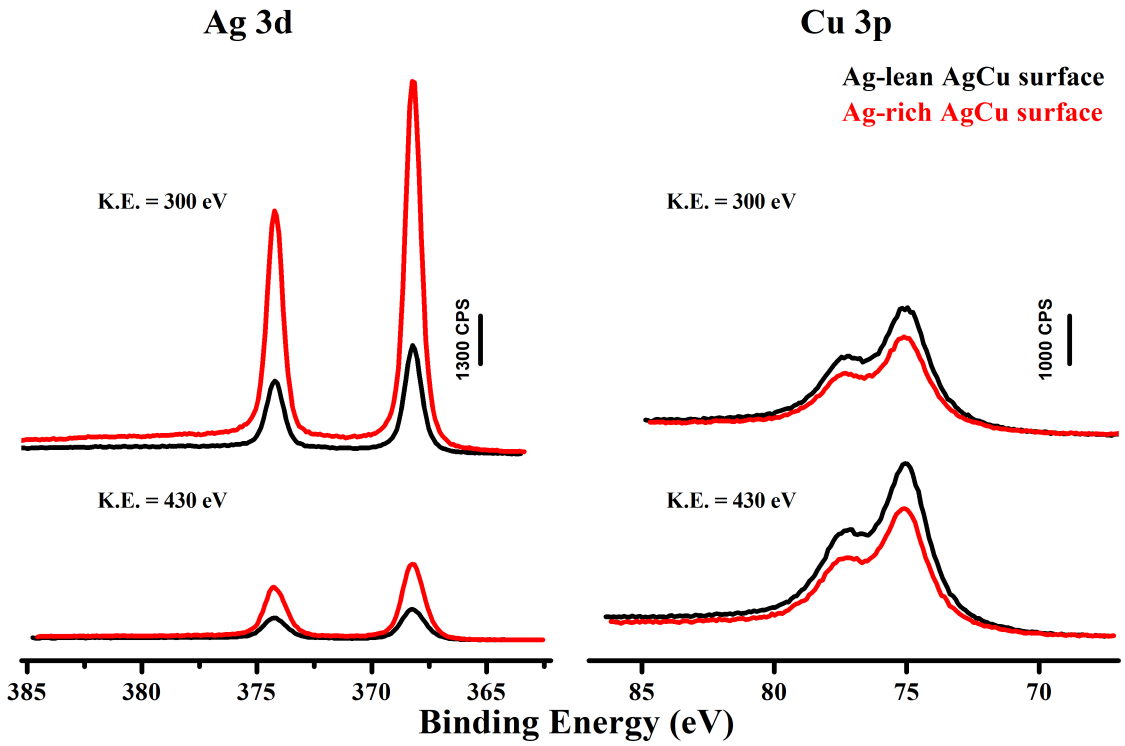

Figure S1. Ag 3d and Cu 3p XPS signals for Ag-rich and Ag-lean surfaces with different photon energies. With different photon energies applied to collect Ag and Cu signals, we can get information with different probing depths. Photon energies of 670 and 800, and 380 and 510 eV, are used to get kinetic energies of 300 and 430 eV for Ag 3d and Cu 3p, respectively. The mean free path for the kinetic energies of 300 and 430 eV are ~0.8 and 1.2 nm, respectively. Applying sensitive factors of each core level under these two kinetic energies and the beam flux correction, the Ag/Cu ratios of the Ag-lean and Ag-rich samples are determined as 0.2:1 and 0.7:1, respectively, at the top ~2.4 nm layer, and they become 0.1:1 and 0.3:1, respectively, at the top ~3.6 nm layer.

The free energy differences initiate the surface evolution

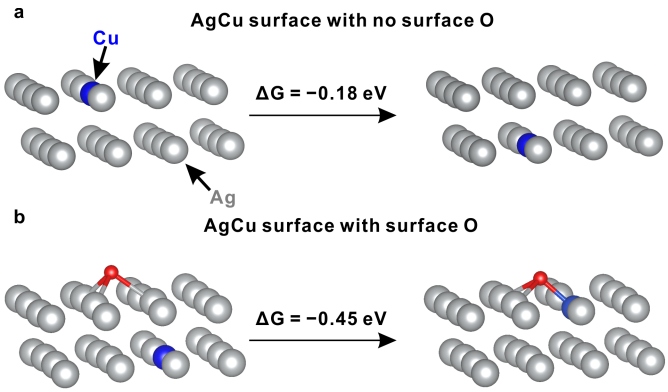

Figure S2. The surface free energy difference with and without surface O. For pristine AgCu surface, having one Cu at surface with respect to having one Cu at subsurface is 0.18 eV less stable, indicating that the AgCu surface is naturally terminated with an Ag layer rather than Cu layer. With one surface O at the three-fold site, the energy difference between having one Cu at surface under the surface O with respect to having one Cu at subsurface is −0.45 eV, indicating that Cu prefers to stay at surface with surface O. The Ag and Cu atoms are presented as grey and blue balls, respectively.

Supporting Information

AgCu component distribution change under various conditions

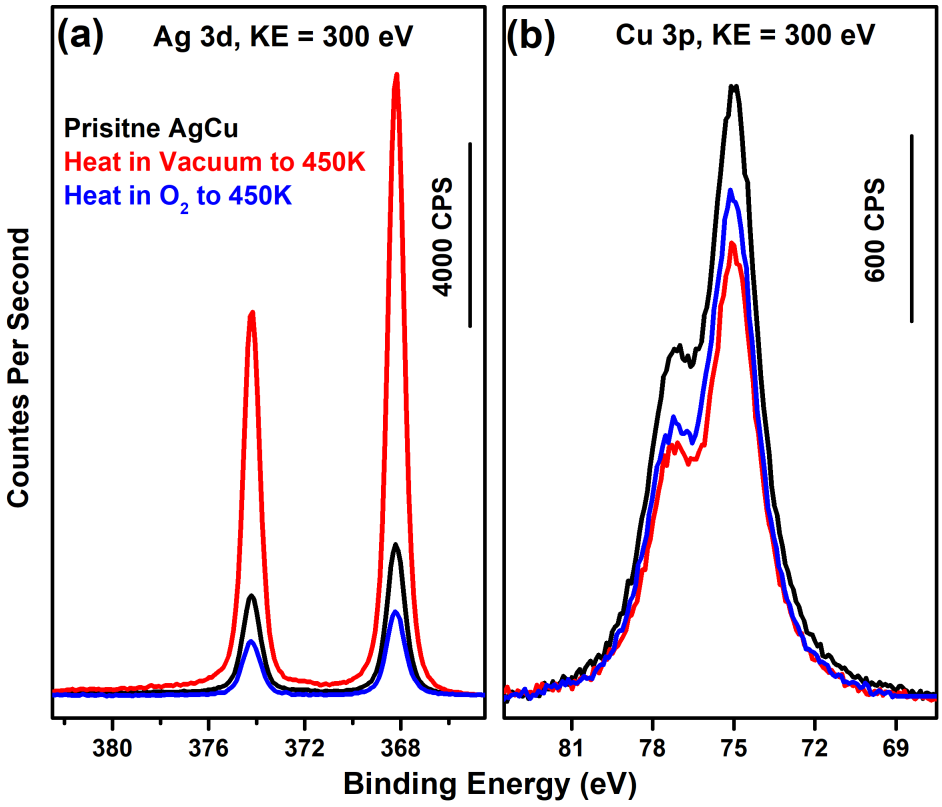

Figure S3. The Ag and Cu distribution changes for different analysis conditions. The Ag 3d and Cu 3p spectra changes were collected with kinetic energy of 300 eV to characterize the component distributions at the top 3.6 nm of sample when heated under 450 K for 5mins at vacuum and with 30 mTorr O_2. The results show that heating the bimetallic sample at vacuum leads to the Ag migration to the surface, while heating with the O_2 leads to the Cu migration to the surface.

Surface O attracting up to three Cu from subsurface to surface

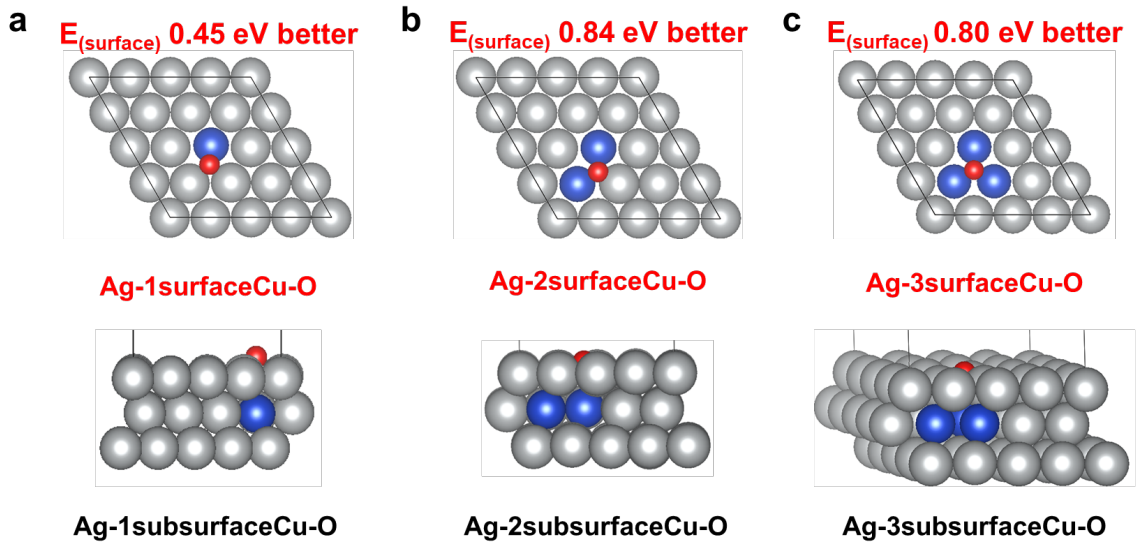

Figure S4. The configurations of up to 3 atoms at subsurface and surface near the surface O. We found that surface O can attract one, two, and three Cu atoms from the subsurface to surface with an energy favorable of 0.45 eV, 0.84 eV, and 0.80 eV, respectively.

Top view, stable adsorbates

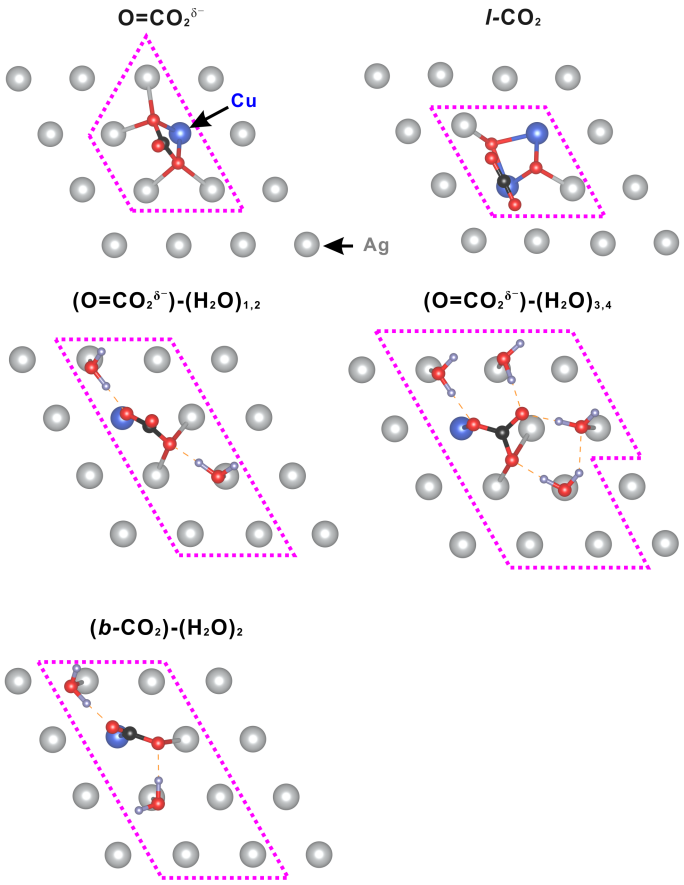

Figure S5. The configuration of adsorbates from CO_2 and H_2O on Ag-Cu matrix illustrated in top view. The configurations of $O{=}CO_2^{\delta-}$, *l*-CO_2, $O{=}CO_2^{\delta-}$ with 1st and 2nd H_2O, $O{=}CO_2^{\delta-}$ with 3rd and 4th H_2O, and *b*-CO_2 with $2H_2O$ are illustrated in top view. The surface catalyst atoms closely interacted with the adsorbates are labeled with pink dash line boxes. These atoms are believed to determine the CO_2 adsorption and activation on the surfaces. $O{=}CO_2^{\delta-}$, *l*-CO_2, $O{=}CO_2^{\delta-}$ with 1st and 2nd H_2O, $O{=}CO_2^{\delta-}$ with 3rd and 4th H_2O, and *b*-CO_2 with $2H_2O$ have closely interactions catalyst atoms of 5, 4, 6, 8, and 6 atoms, respectively. The hydrogen, carbon, oxygen, silver, and copper atoms were represented with light purple, black, red, gray, and blue balls, respectively. The C-O (and C=O), O-H, and hydrogen bonds were represented with black, blue, and orange sticks, respectively. The Ag and Cu atoms are presented as grey and blue balls, respectively.

Surface adsorbates of interests

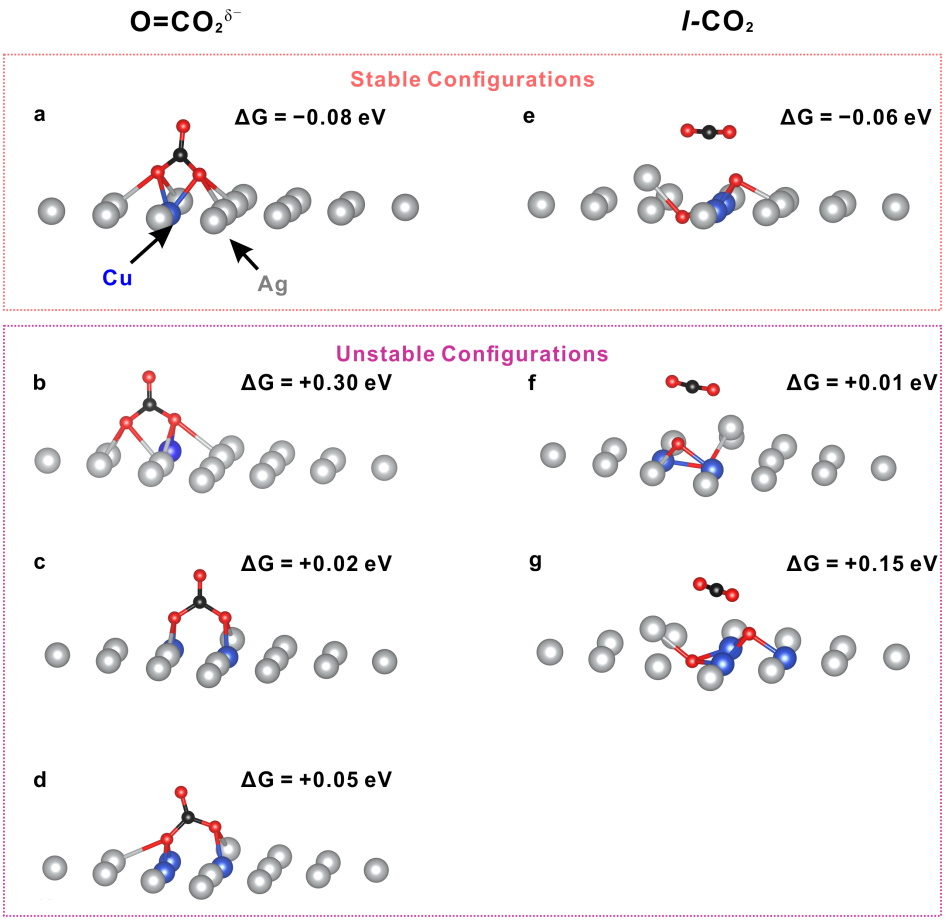

Figure S6. Stable and unstable configurations of $O{=}CO_2^{\delta-}$ and *l*-CO_2 on Ag matrix with Cu dopant. a, The configuration of $O{=}CO_2^{\delta-}$ on AgCu matrix with one Cu dopant under the C atom. This configuration is stable with ΔG = −0.08 eV. **b,** The configuration of $O{=}CO_2^{\delta-}$ on AgCu matrix with one Cu dopant under the O atom. This configuration is unstable with ΔG = +0.30 eV. **c, d,** The configurations of $O{=}CO_2^{\delta-}$ on AgCu matrix with two and three Cu atoms substitution in the Ag matrix. The configurations are unstable with ΔG = +0.02 eV, and +0.05 eV, respectively, for two and three Cu atoms cases. **e,** The configuration of *l*-CO_2 on 2Cu substituted Ag matrix, the CO_2 is perpendicular to the Cu dual atoms. This configuration is stable with ΔG = −0.06 eV. **f,** The configuration of *l*-CO_2 on 2Cu substituted Ag matrix, the CO_2 is parallel with the Cu dual atoms. This configuration is unstable with ΔG = +0.01 eV. **g,** The configuration of *l*-CO_2 on 3Cu substituted Ag matrix. This configuration is unstable with ΔG = +0.15 eV. The Ag and Cu atoms are presented as grey and blue balls, respectively.

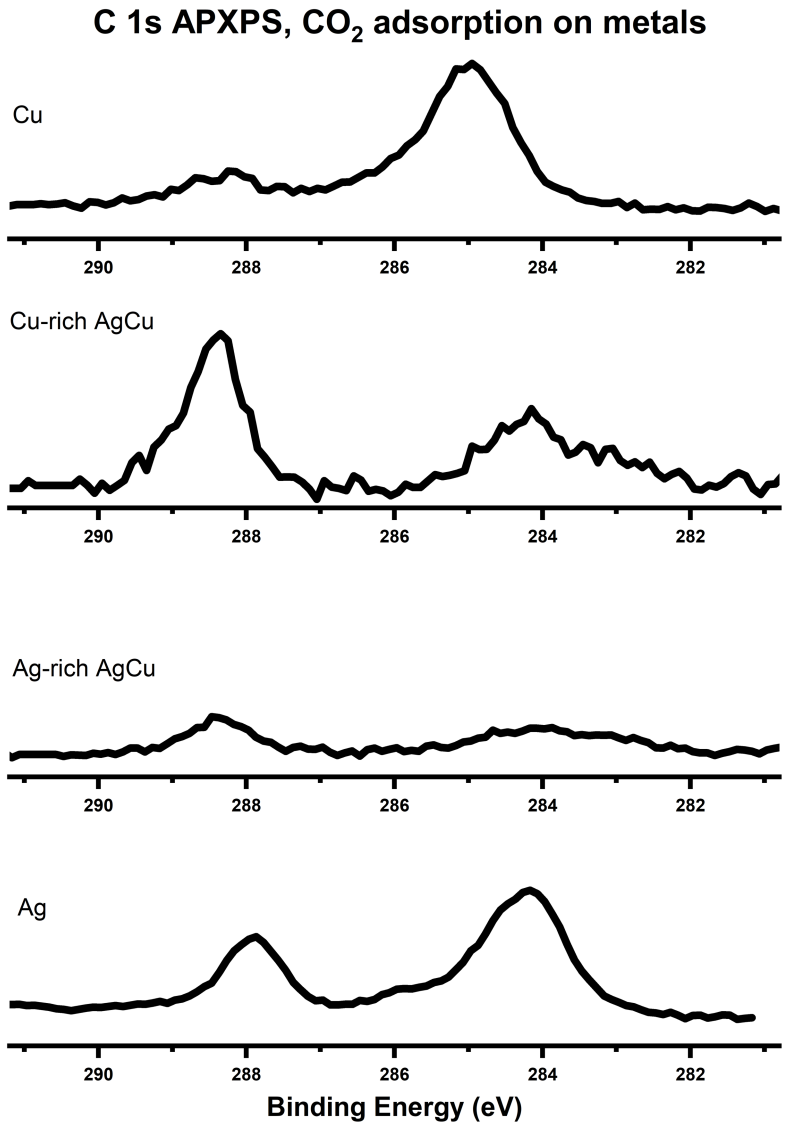

Figure S7. Comparisons of CO_2 adsorption on Ag, Cu, and AgCu surfaces characterized by C 1s APXPS. CO_2 adsorption on AgCu surfaces showed similar spectral profiles with Ag not Cu.

Quantify the surface evolution induced by gas adsorption

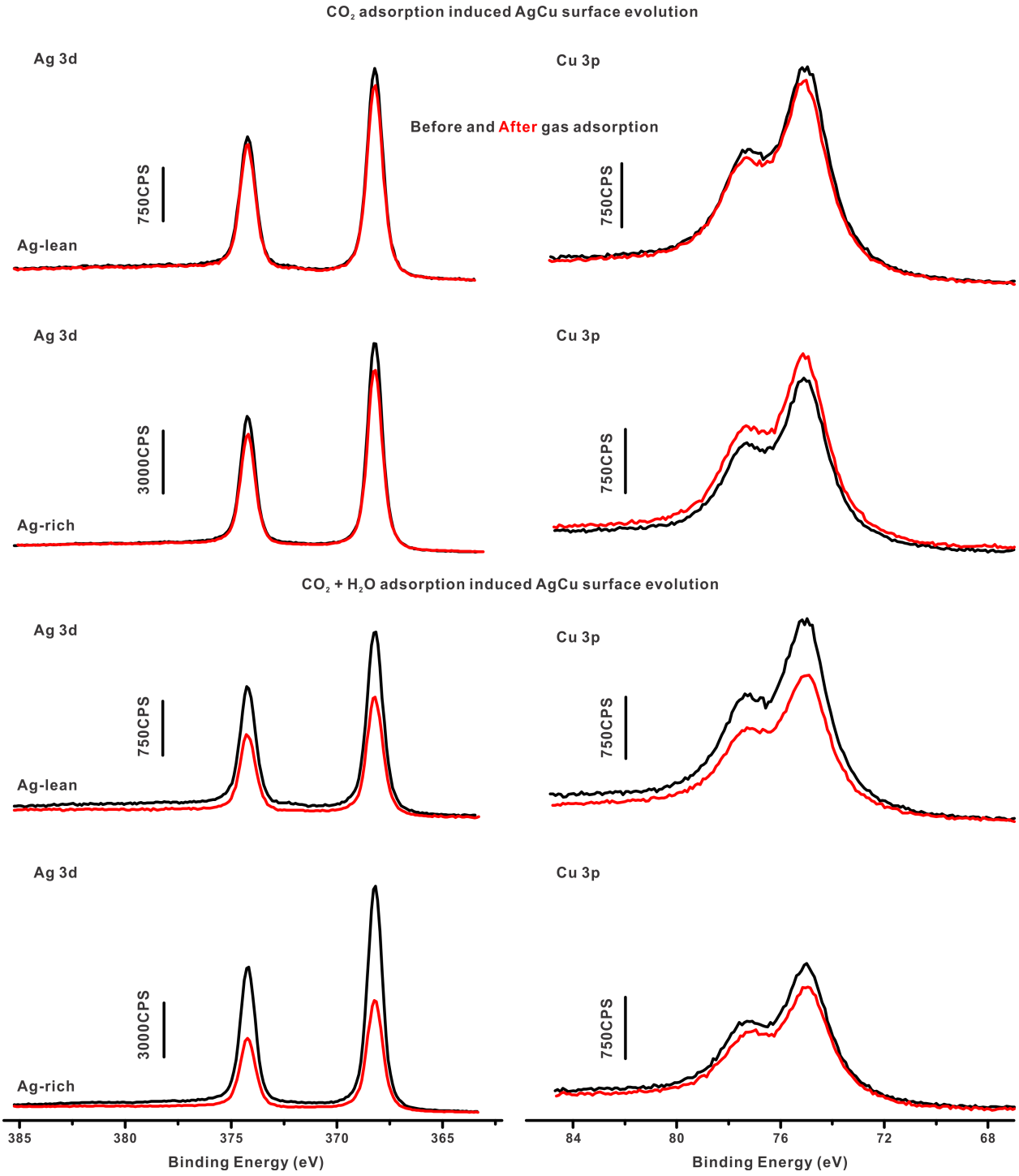

Figure S8. Ag 3d and Cu 3p signals of AgCu surfaces before and after CO_2 adsorption both alone and in the presence of H_2O. The gas adsorption induced surface evolution mainly showing as the Cu migration to surface is monitored by APXPS. The spectra were taken under UHV condition to exclude the influence of the signal attenuation of the gases. The surface adsorbates signals, detecting by C 1s and O 1s spectra, are identified to be unchanged at gas

atmosphere and at UHV condition. The Ag 3d and Cu 3p signals are collected under photon energies of 670 eV and 380 eV to have the same depth profile. The Ag 3d signals show obvious decease after gas adsorption for both surfaces, while Cu 3p signal increase after exposing CO_2 to Ag-rich AgCu surface and decrease for the other cases. The catalyst signals do not show the same attenuation level, indicating the surface reconstruction induced by the gas adsorption.

Supporting Information

O signals on AgCu surface after adsorption tracked by APXPS

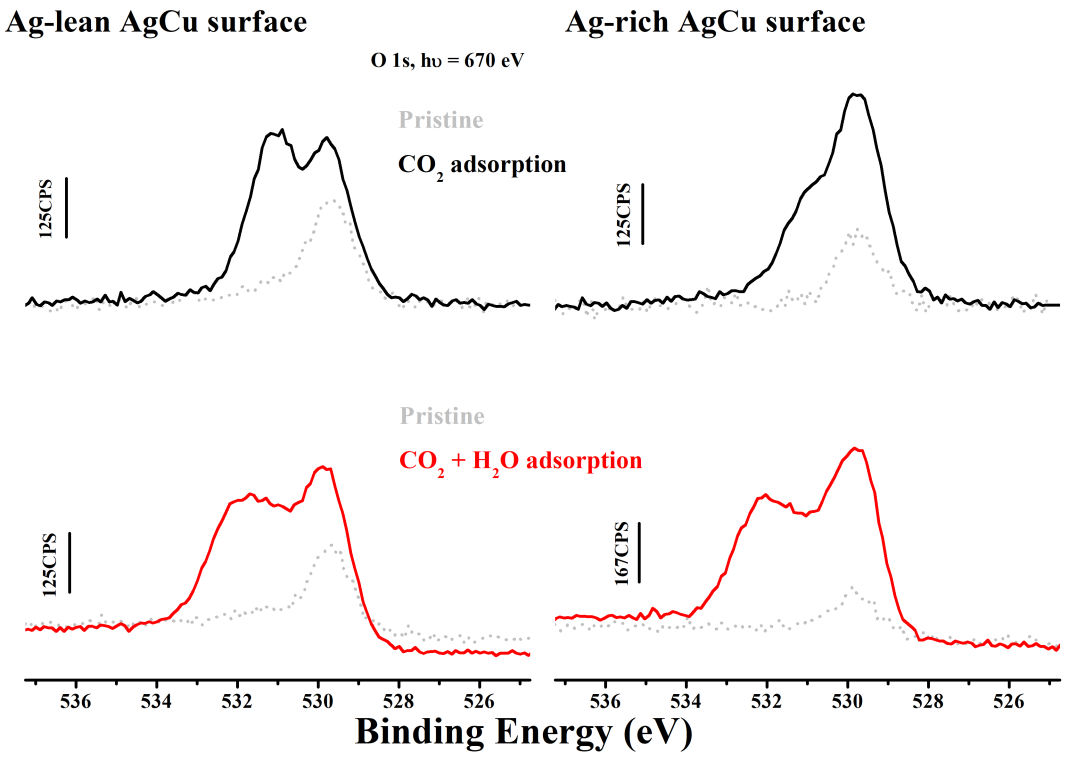

Figure S9. O1s spectra of AgCu surface with CO_2 and CO_2+H_2O adsorption. The O 1s spectra recorded on Ag-rich and Ag-lean AgCu surfaces with CO_2 and CO_2+H_2O adsorption. For comparison, the pristine surfaces are shown as grey dash lines, while the adsorbed surfaces are shown as red lines. The O 1s locating at ~529.8 eV represents the surface O on AgCu surface.

CO_2 adsorption on oxidized AgCu surface

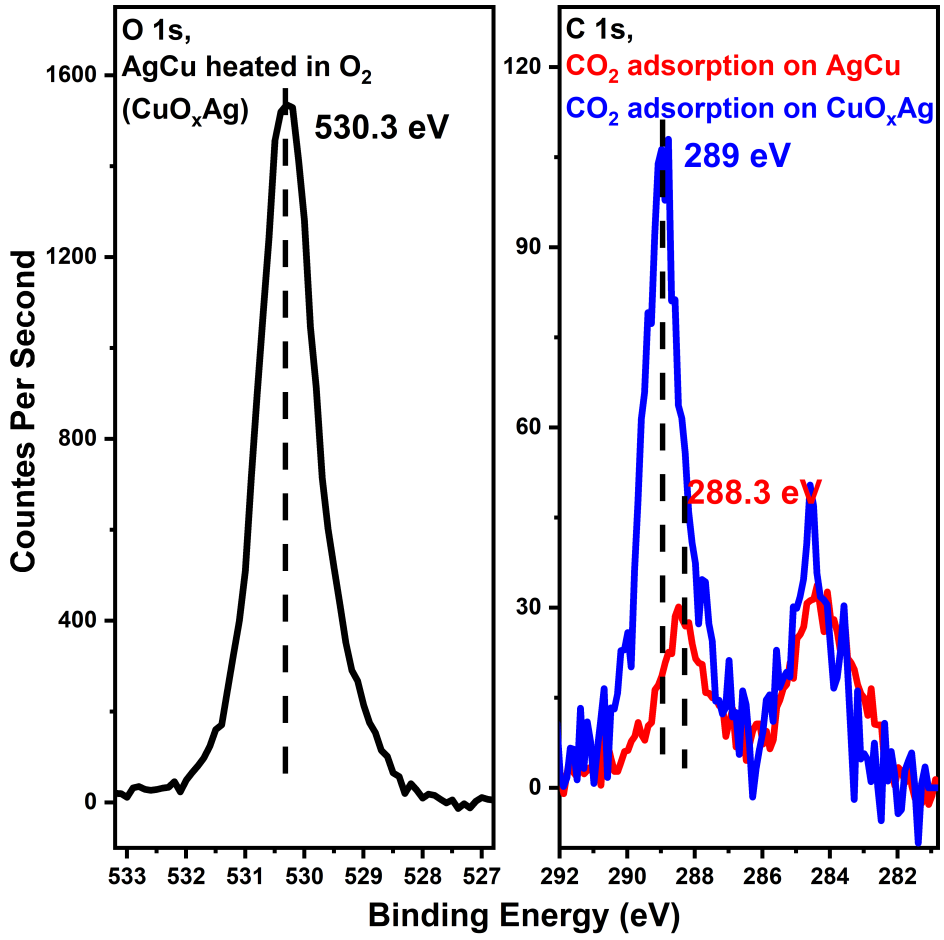

Figure S10: O1s spectra of AgCu surface heated in 30 mTorr O_2 at 450 K for 5mins, and C 1s spectra of CO_2 adsorption on AgCu surface and AgCu surface heated in O_2. We observed the O 1s peak locating at 530.3 eV after AgCu heat treated in O_2, indicating the formation the CuO_x. Thus, we concluded that heating AgCu in 30 mTorr O_2 at 450 K leads to the formation of a CuO_x layer on top of AgCu, denoting as CuO_xAg. CO_2 adsorption on this CuO_xAg surface leads to a C 1s peak appearing at around 289 eV, showing a blue shift with respect to the adsorbate peak of CO_2 adsorption on pristine AgCu surface. The peak at 289 eV corresponds to the ionic carbonate.

Supporting Information

References:

(1) McClurg, R. B.; Flagan, R. C.; Goddard, W. A., III *J. Chem. Phys.* **1997**, *106*, 6675– 6680, DOI: 10.1063/1.473664

(2) Campbell, C. T.; Sprowl, L. H.; Árnadóttir, L. *J. Phys. Chem. C* **2016**, *120*, 10283– 10297, DOI: 10.1021/acs.jpcc.6b00975

(3) Redondo, A.; Zeiri, Y.; Goddard, W. A., III *Phys. Rev. Lett.* **1982**, *49*, 1847, DOI: 10.1103/PhysRevLett.49.1847

(4) Köhler, L., & Kresse, G. (2004). *Physical Review B*, *70*(16), 165405.